Hindawi Publishing Corporation
Advances in Mechanical Engineering
Volume 2013, Article ID 340435, 13 pages
http://dx.doi.org/10.1155/2013/340435

Research Article

Modelling, Simulations, and Optimisation of Electric Vehicles for Analysis of Transmission Ratio Selection

Paul D. Walker,[1] Salisa Abdul Rahman,[2] Bo Zhu,[1,3] and Nong Zhang[1]

[1] *School of Electrical, Mechanical, and Mechatronic Systems, Faculty of Engineering and Information Technology, University of Technology, Sydney, P.O. Box 123, Broadway, Sydney, NSW 2007, Australia*
[2] *Department of Physical Science, Faculty of Science and Technology, Universiti Malaysia Terengganu, 21030 Kuala Terengganu, Malaysia*
[3] *BAIC Motor Electric Vehicle Co. Ltd., Chaoyang District, Beijing 100021, China*

Correspondence should be addressed to Paul D. Walker; paul.walker@uts.edu.au

Received 21 August 2013; Accepted 18 October 2013

Academic Editor: Yuan Zou

Pure electric vehicles (PEVs) provide a unique problem in powertrain design through the meeting of performance specifications whilst maximising driving range. The consideration of single speed and multispeed transmissions for electric vehicles provides two strategies for achieving desired range and performance specifications. Through the implementation of system level vehicle models, design analysis, and optimisation, this paper analyses the application of both single speed and two-speed transmission applications to electric vehicles. Initially, transmission ratios are designed based on grade and top speed requirements, and impact on vehicle traction curve is evaluated. Then performance studies are conducted for different transmission ratios using both single speed and two-speed powertrain configurations to provide a comparative assessment of the vehicles. Finally, multivariable optimisation in the form of genetic algorithms is employed to determine an optimal gear ratio selection for single speed and two-speed PEVs. Results demonstrate that the two-speed transmission is capable of achieving better results for performance requirements over a single speed transmission, including vehicle acceleration and grade climbing. However, the lower powertrain efficiency reduces the simulated range results.

1. Introduction

Through the development alternative powertrain technologies there has been a trend towards the development of hybrid electric and pure electric vehicles (PEVs), reducing fossil fuel consumption through higher powertrain efficiencies. Popular PEVs, such as those presented in [1, 2], utilise either single ratio transmissions or direct drive with no gear reduction to deliver traction load to the road. Consequently, gear ratio design requires achieving a balance between range, performance, and top speed. Highlighted in [2] early PEVs have a range of approximately 80 km and top speed of 65 km/h, as compared to the car presented in [1], with a range of 160 km and top speed of 130 km/h. Such improvements in vehicle performance are a result of increased energy density in current battery technologies and motor efficiency. This paper addresses this design issue through the application of a two-speed transmission to PEVs.

As PEVs have a much simpler powertrain arrangement when compared to hybrid and conventional powertrains, with the electric machine (EM) either directly driving the wheels or using a single speed reduction ratio [1, 3–5], the motor must deliver power over a very wide speed range, that is, high power at low speed to maximise acceleration performance and at high speed to overcome higher aerodynamic drag losses. The use of single speed or direct drive motors requires a larger motor with wide torque and speed ranges to achieve both of these objectives. Much like a conventional powertrain, by using multiple gear ratios, it is possible to improve the useful torque and speed range of the EM without increasing motor size. This strategy is frequently employed in HEVs and plug-in HEVs (PHEVs), such as those reported in [6, 7], where it is quite common to make use of smaller EMs operating in conjunction with ICEs.

Design analysis of hybrid and electric vehicles is achieved through the development of system level models integrating power sources (batteries and capacitors), driving components (engines, motors), and vehicle driveline (transmission, wheels) models. Structuring these models is highly dependent on the focus of research, be it component design [8], energy analysis [3, 6, 9], or system optimisation [10]. Different modelling scenarios and strategies are discussed in [11] for a range of novel powertrain configurations. Model development of vehicles powertrains provides a significant step in moving from concept analysis through to prototyping and development and allows for the flexibility when conducting detailed studies of the powertrain of interest.

An emerging application of system level vehicle models is design optimisation, typically realised through model-in-the-loop strategies. Optimisation strategies are a powerful tool for the identification of the best possible solutions to design problems, particularly when conflicting demands may not provide a directly identifiable optimal solution. Such methods have proven to be very successful in the configuration of hybrid powertrains and respective energy management strategies [10, 12–14]. Genetic algorithm (GA) optimization [15–18] is a process of searching the minimum or maximum limits of an objective function while at the same time satisfying certain constraints on the design variables and also selecting the best configurations resulting from each generation. A model-in-the-loop approach is used in the design optimization process in this paper, as illustrated in Figure 1. As shown in the middle of the diagram, the PEV powertrain is modelled in MATLAB/Simulink as the simulation tool. In this process, the objective functions are evaluated through results obtained from the simulation.

The purpose of this paper is to develop a thorough understanding of how gear ratios are selected for electric vehicle transmission design and how this selection impacts on overall vehicle performance. To achieve this the paper develops compact single speed and two-speed electric vehicle system models for the evaluation of vehicle performance and provides optimised transmission specifications that provide maximum vehicle range while still meeting desired vehicle performance characteristics. The rest of this paper is divided as follows. Section 2 provides details of the PEV model. Section 3 details selection of transmission ratios through traditional design methodologies, and Section 4 provides simulations to study how these ratios impact on performance for single speed and two-speed transmissions. Optimization using genetic algorithms is undertaken in Section 5, providing simulation and optimisation results for single speed and two-speed transmissions and enabling detailed comparison of the two transmissions. Finally, in Section 6 the work is summarised and concluding remarks are conveyed.

2. PEV Model

In electric vehicles both mechanical and electrical systems are designed to provide optimal range and performance. The MATLAB/Simulink model of the PEV powertrain uses a bottom-up modelling strategy where the difference between desired and acquired vehicle speeds defines power demand from the driver; this demand is matched by the battery to supply the motor and drive the vehicle. Table 1 summarizes the vehicle parameters for a large passenger sedan based on the Beijing Electric Vehicles (BJEV) C40B, a class D passenger vehicle.

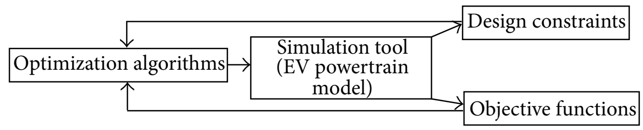

Figure 1: Model-in-the-loop design optimization process.

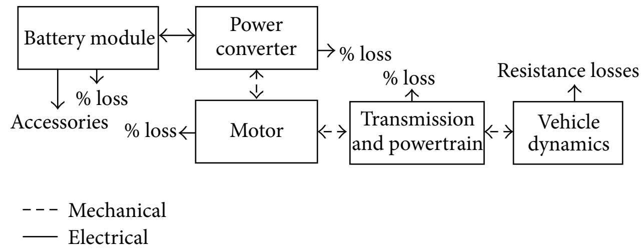

Figure 2: Electric vehicle power flow.

Table 1: Vehicle parameters.

Vehicle parameter	Units	Quantity
Mass	Kg	1780
Wheel radius	m	0.32165
Drag coefficient	—	0.28
Frontal area	m^2	2.2
Rolling resistance coefficient	—	0.016
Powertrain efficiency	—	0.8
Inverter efficiency	—	0.95
Battery (Li-ion 1p120s)	Ah (V)	26 (360)
Motor (peak)	kW (Nm)	75 (250)
Motor (nominal)	kW (Nm)	40 (135)

The flow of power in the PEV considers stored battery energy, electrical energy delivered to the motor, conversion of electrical energy to mechanical in the motor, and the delivery of mechanical one energy to the wheel via the transmission, whilst for energy recovery the process is reversed. Each of these steps of energy delivery results in power loss through mechanical and electrical inefficiencies. The nature of power flow for the PEV is shown in Figure 2. Each of these subsystems is modelled in the following sections.

2.1. Battery. Simulation of the battery considers calculation of output voltage, state of charge (SOC), and battery temperature. The battery pack is modelled around individual cells and then multiplied together to determine the total battery pack voltage during discharging and charging, as indicated in (1) to (6). The battery current (I) is calculated as a function of demand power (P_D) and battery output voltage (V_{out}) as follows:

$$I = \frac{P_D}{V_{OUT}}. \quad (1)$$

Thus, V_{OUT} is considered the actual voltage across the battery module which is either supplying the motor or supplied to the battery when the motor is acting as a generator. The cell open circuit voltage (V_{OC}) and internal resistance for charging ($R_{INT,CHARGE}$) and discharging ($R_{INT,DISCHARGE}$) are modelled using lookup tables as a function of temperature (Temp) and state of charge (SOC)

$$V_{OC} = V_{OC,Cell}(\text{Temp}, \text{SOC}) \times B_{CELLS}. \quad (2)$$

The internal resistance of the batteries during charging and discharging is

$$R_{INT,CHARGE} = R_{INT,CHARGE}(\text{Temp}, \text{SOC}) \times B_{CELLS}, \quad (3)$$

$$R_{INT,DISCHARGE} = R_{INT,DISCHARGE}(\text{Temp}, \text{SOC}) \times B_{CELLS}. \quad (4)$$

The output voltage of the battery pack during charging and discharging is

$$V_{OUT,CHARGE} = V_{OC} - R_{INT,CHARGE} \times I, \quad (5)$$

$$V_{OUT,DISCHARGE} = V_{OC} - R_{INT,DISCHARGE} \times I \times \eta_C. \quad (6)$$

State of charge (SOC) calculation is an iterative process dependent on power demand from the motor or power supply from regenerative braking. The rate of current supply is taken from the initial capacity of the battery and absolute SOC determined, based on change over time from initial SOC. State of charge range is taken from the original BJEV platform with a minimum SOC of 10% and maximum SOC of 90%.

Maximum battery capacity (CAP_{MAX}) is determined from the battery configuration and is temperature dependent and the used capacity (CAP_{USED}) from supply or demand of the EM. The absolute SOC is defined as

$$\text{SOC} = \frac{(CAP_{MAX} - CAP_{USED})}{CAP_{MAX}}. \quad (7)$$

A simple heat transfer model is used to evaluate heating and cooling of the batteries as required. The thermal model uses the heat generated from internal resistance to heat the battery and convection of an individual cells surface provides cooling. Two cases of convection are employed: (1) free convection if the battery temperature is below the minimum required for cooling and (2) forced convection if active cooling is required. It is assumed that the temperature of each cell is equal throughout the battery pack. The heat energy (E_{CELL}) created in a battery cell results from the current supplied to the cell multiplied by the internal voltage in the cell:

$$E_{CELL} = \frac{(V_{OC} - V_{OUT}) \times I}{B_{CELLS}}. \quad (8)$$

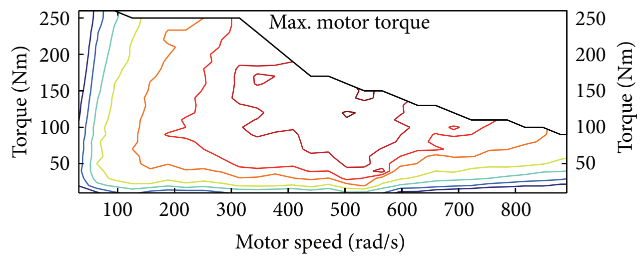

Figure 3: Maximum torque and efficiency plots of the electric machine.

The heat lost from each cell is determined through free and forced convection (E_{COOL}) as

$$E_{COOL} = hA_{CELL}(T_{CELL} - T_{AMB}). \quad (9)$$

For the convection coefficient, h is dependent on free convection or forced convection with cooling of the cells. The difference between energy generated and energy lost through convection results in heating of the battery cell. The temperature of the cell (T_{CELL}) is, with M_{CELL} being mass of each cell and CP_{CELL} being the specific heat, then

$$T_{CELL} = \int \frac{E_{CELL} - E_{COOL}}{M_{CELL} CP_{CELL}} \text{dt}. \quad (10)$$

2.2. Electric Machine (EM). The EM is a permanent magnet alternating current unit with peak and nominal torque and speed detailed in Table 1. It provides both driving and regenerative braking functionalities for the vehicle. The electric machine accepts input power from power converter and batteries (11), which is then converted to output torque in (12) by dividing it by motor speed; finally motor efficiency loss is calculated from the motor efficiency map (Figure 3) and torque of the transmission is determined. Figure 3 presents the efficiency map of the 75 kW permanent magnet AC motor.

Acting as a driving motor the power supplied from the batteries is converted to motor power; this is used to calculate motor torque through division by the motor speed and limited by the maximum torque of the motor

$$P_{EM} = \eta_{PC} \eta_{EM} P_D, \quad (11)$$

where P_{EM} is electric machine power, η_{PC} is power converter efficiency, and electric machine efficiency is $\eta_{EM} = f(\omega_{EM}, T_{EM})$. EM torque ($T_{EM}$) is a function of EM power and speed (ω_{EM}) or vehicle speed (ω_V) and engaged gear ratio (γ):

$$T_{EM} = \frac{\eta_{PT} P_{EM}}{\omega_{EM}} = \frac{\eta_{PT} P_{EM}}{\gamma \omega_V}. \quad (12)$$

During regenerative braking, battery charging power (P_B) is used to estimate the torque in the generator by dividing the battery demand by motor speed and is limited by the maximum torque from the torque curve. This produces an estimated generator power which is multiplied by the EM and power converter efficiency to determine actual power supplied to the battery module

$$P_B = 0.3\eta_{PC}\eta_{EM}P_{EM}, \tag{13}$$

$$P_{EM} = \eta_{PT}T_{EM}\omega_{EM} = \eta_{PT}T_{EM}\gamma\omega_V. \tag{14}$$

2.3. Transmission. For these simulations a simple transmission model is used, where, according to the defined shift map from vehicle speed and motor torque, required gear, G1 or G2, is selected. Separate maps are required for up- and downshifts. For this model only the overall gear ratio is provided; the final drive ratio must be divided into the output ratios to determine actual gear ratio. Shift logic for the transmission proceeds as follows.

(1) For the upshift logic the vehicle speed is used to determine the target torque for shifting; if motor torque is less than the target torque an upshift is initiated as the motor is in a lower efficiency region.

(2) Alternatively, for the downshift, using the downshift map, if motor torque exceeds the target torque, the motor is now in a low efficiency region and a downshift is initiated.

(3) For braking events, similar logic as described above follows, such that, once motor speed is too low, the highest ratio is selected.

(4) If the vehicle is stopped, the shift map is overridden and the first gear is selected.

2.4. Vehicle. The vehicle model takes all the input torques, calculates vehicle acceleration and performs numerical integration to determine vehicle speed. Thus a single degree of freedom representing torsional equivalent vehicle inertia is used in place of the linear system, and conversion between rotational and linear systems is completed after integration. Inputs are supplied motor/generator torque, brake torque, and vehicle resistance torque, and the output is vehicle speed. Equation of motion for the vehicle is

$$M_V r_t^2 \alpha = \eta_{PT}T_{EM} \cdot \gamma - T_V - T_B, \tag{15}$$

where r_t is the tyre radius and M_V is vehicle mass. The vehicle resistance torque, T_V, is the combination of rolling resistance loss, incline load, and air drag loss, T_B is mechanical brake torque, this is defined in the braking model section, and η_{PT} is the powertrain efficiency. Resistance forces are converted to a torque through multiplication by the tyre radius. Vehicle resistance torque is defined as

$$T_V = \left(C_R M_v g \cos\emptyset + M_V g \sin\emptyset + \frac{1}{2}C_D \rho A_V V_V^2\right) \times r_t, \tag{16}$$

where C_R is rolling resistance, g is gravity, $\emptyset$ is road incline angle, C_D is drag coefficient, ρ is air density, A_V is frontal area, and V_V is linear vehicle speed.

2.5. Mechanical Braking. The integration of mechanical and regenerative braking is strategically important to maximise the energy recovered whilst maintaining passenger safety. To simulate this successfully the required brake torque is estimated from the driver demand model in the controller and mechanical braking is portioned depending on braking requirement. Regenerative braking and mechanical braking are proportioned as follows.

(1) If demand brake torque exceeds regenerative brake torque, apply mechanical brakes to meet difference in torque limits.

(2) If vehicle speed is less than 15 kph, apply mechanical braking only.

This produces a brake model that is a function of driver demand, regenerative braking, driving conditions, and brake torque limit. Under regenerative braking conditions brake torque is calculated as

$$T_B = \frac{P_D}{\omega_V} - \gamma T_{EM}. \tag{17}$$

Below the 15 kph limit, with a limiting torque, it is calculated as

$$T_B = \frac{P_D}{\omega_V}. \tag{18}$$

2.6. Driver. The driver is modelled as a PID controller, where the difference between desired and actual vehicle speed is used to output the demand power. Based on these speeds and the demanded power, the vehicle state is determined as either accelerating, braking, or stopping. This drives the EM, transmission, and battery module operation.

3. Ratio Design for Electric Vehicles

3.1. Ratio Design for Grade. The design of gear ratios for the capability to climb inclines is considered important for entering and leaving steep driveways and parking structures. The largest overall gear ratio required for the powertrain is set based on the ratio of rolling resistance for a specified grade of 30% divided by the maximum motor torque multiplied by the overall powertrain efficiency; this is given in (19) [19]. For low speeds the aerodynamic drag is assumed to be zero. Here the maximum motor torque T_{EM} is 260 Nm. Consider

$$\gamma_{max} = \frac{r_t m_V g\left(C_R \cos\Phi + \sin\Phi\right)}{\left(T_{EM}\eta_{PT}\right)}. \tag{19}$$

This produces a minimum ratio of 8.17 for the first gear to achieve a 30% grade climb at low speed.

3.2. Ratio Design for Speed. Vehicle top speed varies significantly depending on application and is reasonably important for consumer acceptance. The maximum speed achieved in the vehicle can then be used to determine the lowest possible ratio. It must consider the motor characteristics in terms of maximum rotating speed (N_m) and the ability of the motor torque to reach this top speed. The minimum ratio is defined by the maximum motor speed [19], converted to kph divided by the maximum vehicle speed

$$\gamma_{\text{min,speed}} = \frac{3.6\pi N_m r_t}{(30 v_{\max})}. \quad (20)$$

The resulting ratio is $\gamma_{\text{min,speed}} = 5.7$. This ratio can be checked against the capability of the motor to supply torque at this speed by dividing the rolling resistance and aerodynamic drag by the maximum motor torque at its maximum speed:

$$\gamma_{\text{min,torque}} = \frac{\left(C_R m_v g \cos\emptyset + (1/2) C_D \rho A_V V_V^2\right) \times r_t}{\left(\eta_{\text{PT}} T_{\text{EM,@maxRPM}}\right)}. \quad (21)$$

The resulting ratio is $\gamma_{\text{min,torque}} = 5.12$, suggesting that the motor is capable of supplying torque at the maximum vehicle speed for gear ratios including the design ratio of 5.7.

3.3. Traction Curve. Traction curves can be used to demonstrate how multiple transmission gear ratios can effectively increase the operating functionality of PEV electric machines and are frequently used to study the application of ICE loads in conjunction with transmission ratio; see [19] for details on traction load. This curve is defined using the maximum motor power as follows:

$$F_T = \eta_{\text{PT}} \frac{P_{\max}}{V}. \quad (22)$$

The adhesion limit is the force required for the wheels to transit from rolling to sliding, and for a front wheel drive it is a function of C_W weight distribution and μ_S tyre static friction coefficient

$$F_A = C_W \mu_S g M_v. \quad (23)$$

As a function of vehicle speed, tractive load is a hyperbolic curve and represents the theoretically maximum tractive load delivered by the EM to the wheels. For conventional vehicles the maximum load is available for only a very small region in each gear; thus many gear ratios are required to achieve the best possible use of the engine. For EMs with constant power regions the maximum tractive load can be delivered over a wider region, and fewer gears are required. The application of a two-speed transmission can be used to increase the range of applied load to maximise top speed and increase the maximum tractive force to improve acceleration and grade climbing capabilities. In Figures 4(a) and 4(b) the tractive loads are shown for the EM driving the vehicle through both gears 1 and 2 for maximum power and nominal power output, respectively. This demonstrates clearly the effects of conflicting performance requirements on ratio selection, where for higher ratios (i.e., gear 1) higher load is delivered to the road, at a cost of top speed, reaching approximately 100 kph only. Whilst using lower ratios (i.e., gear 2), a significantly higher speed is achieved at a cost of road load and vehicle acceleration.

Table 2: Vehicle performance simulation for single speed and two-speed transmission EV.

Parameter	Units	Two-speed	One-speed	
Gear ratio(s)		5.7/8.17	8.17	5.7
Powertrain efficiency	—	0.8	0.9	0.9
Range HWFET	km	141.5	151.2	157.3
Range UDDS	km	129.9	142.1	140.2
Acceleration 0–100 km/h	s	14.5	11.6	13.5
Acceleration 0–60 km/h	s	6.3	4.8	6.5
Acceleration 50–80 km/h	s	4.7	4.0	4.2
Grade climbing	%	30	34	23
Top speed	Km/h	180	126	180

4. Comparison of Single Speed and Two-Speed EV Powertrain Performance

The key consideration that divides single speed and two-speed transmissions is the difference in efficiencies between single speed and multispeed transmissions, for a multi-speed automatic transmission efficiencies trend in the region between 85 and 95% [20]. Contributions to these losses include friction and spin losses in the gear train and associated components and the need to power hydraulic control components. Through the inclusion of other losses such as differential and additional power consumed through the control system, the efficiency in Table 1 is assumed to be representative of overall loss in the two-speed drivetrain. As a single speed has a simple transmission design and few components, the vehicle mass is reduced to 1720 kg, and the powertrain efficiency is increased to 90%. Simulations are conducted using both the highway fuel economy driving schedule (HWFET) and the urban dynamometer driving schedule (UDDS) drive cycles. HWFET is considered to be a reasonable approximation of highway style driving, whilst UDDS is associated with city style driving.

Shown in Table 2, the simulated performance outcomes demonstrate the flexibility achieved from the application of a two-speed PEV. A range of successful results including grade climbing, top speed, and acceleration are clearly demonstrated. These are complemented by the simulated range results; whilst the two-speed has poorer range with lower overall efficiency, it is still capable of achieving a similar range. Single speed transmission results clearly indicate that the lower ratio of 5.7 provides increased range performance at high speed driving at a cost of acceleration and grade climbing capability. In comparison to the two-speed transmission simulation results (Table 2, Figures 5 and 6), the application of a single speed transmission is underperformed either in range and top speed requirements or in acceleration and grade climbing capability, depending on the chosen ratio for the transmission.

Figures 5 and 6 demonstrate the results for UDDS and HWFET simulations, respectively. Results in Figures 5(a) and 5(b) present the vehicle speed and engaged gear graphics, demonstrating gearshift repeating as demanded by the shift schedule. It is noticeable that the demand for gear shift occurs

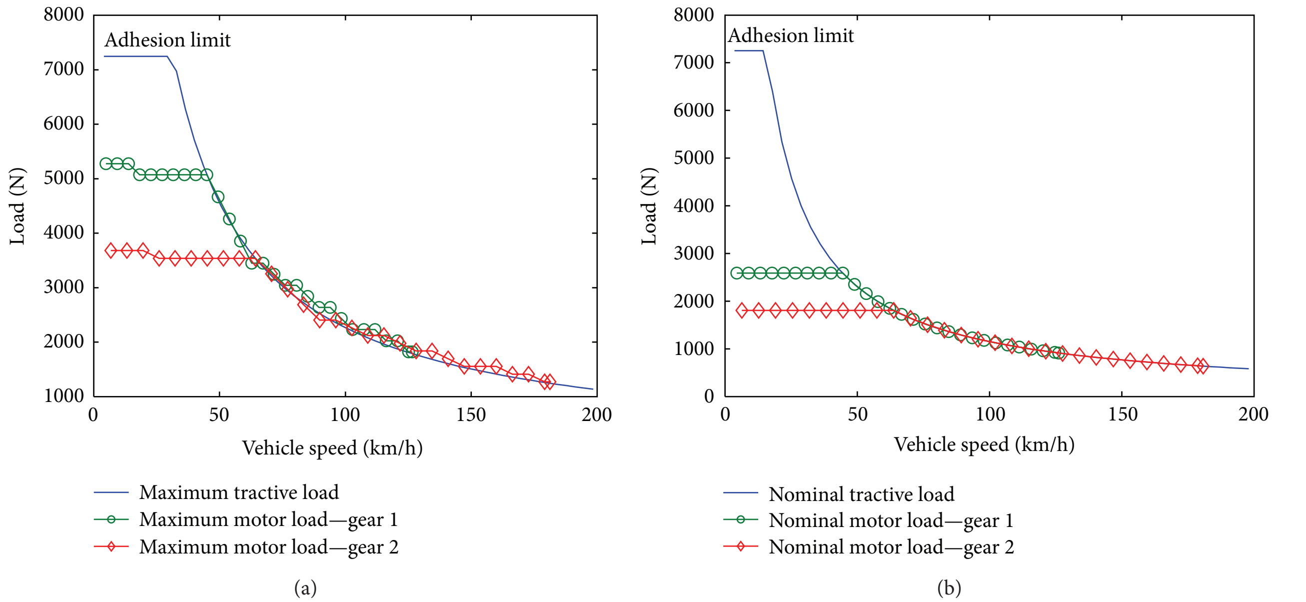

Figure 4: Traction curves for an electric vehicle at (a) maximum power and (b) nominal power using designed gear ratios (gear 1 = 8.17 and gear 2 = 5.7).

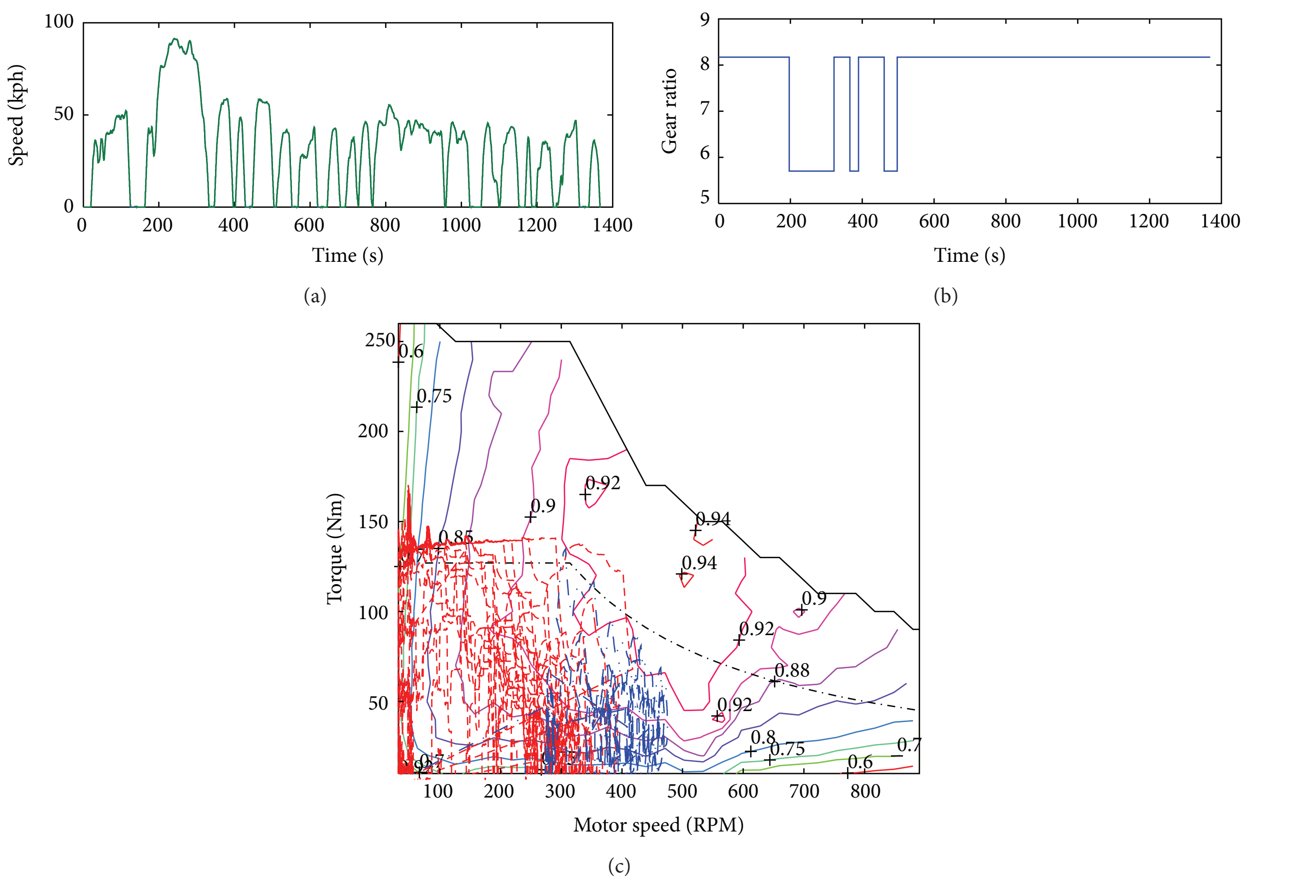

Figure 5: Simulations results for one UDDS drive cycle, (a) vehicle speed, (b) engaged gear ratio, and (c) motor torque and speed trace (red is gear 1; blue is gear 2).

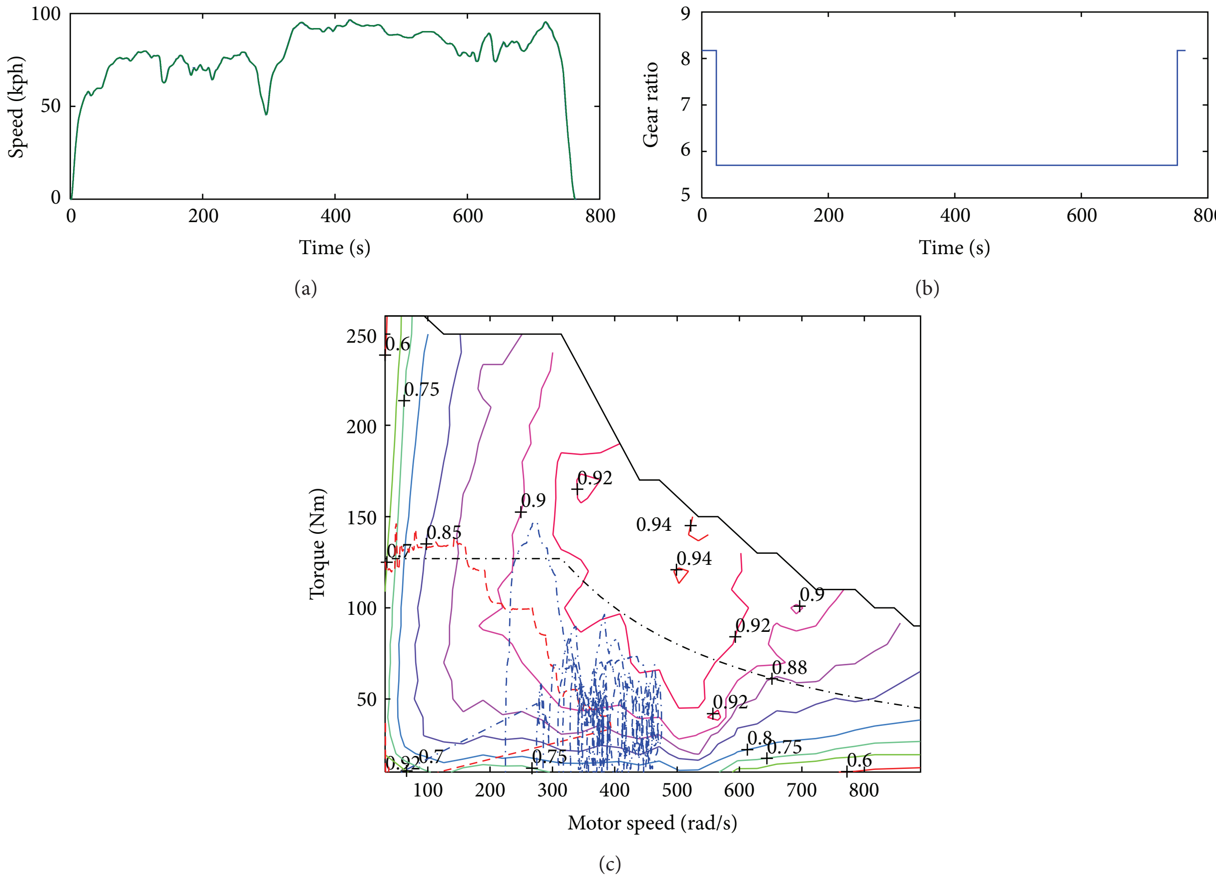

Figure 6: Simulations results for one HWFET drive cycle, (a) vehicle speed, (b) engaged gear ratio, and (c) motor torque and speed trace (red is gear 1; blue is gear 2).

infrequently, predominantly as UDDS cycle is primarily a low speed drive style and the shift region for upshifting is above about 55 km/h. In Figure 5(c) the motor speed trace of torque against speed is shown such that the operating condition of the motor can be studied. It is demonstrated here that, while the motor is operating in a wide range of driving conditions, the operating region is not optimal. A more preferential region between 300 and 600 rad/s is obvious based on the motor efficiency map; see Figure 3. The gear changes into the second gear also show that the EM operating region is reasonable, in comparison to the first gear. The motor trace results in Figure 6(c) indicate that the operating region for the second gear is reasonable for this drive cycle but not necessarily optimal.

Single speed transmission results are demonstrated in Figure 7, employing both designed ratios as a continuously engaged reduction gear for the transmission. Figures 7(a) and 7(b) demonstrate the operating region under a UDDS cycle for the two designed ratios. Particularly, they demonstrate that using a higher ratio, designed for top speed, requires additional torque whilst under low speed with high acceleration demand. This leads to frequent excursions above the nominal torque curve, suggesting that the design ratio is inadequate for city drive cycles. In Figure 7(a) there is clear indication that the ratio is underdesigned and a higher gear ratio will push the motor into a better operating region. Figures 7(c) and 7(d) are simulation results under the HWFET drive cycle. Simulation results with the highest gear ratio of 8.17 demonstrate that the motor drive is well outside what should be expected for the ideal drive region, frequently driving the vehicle with motor speeds above 7000 RPM. Conversely, Figure 7(d) shows the motor operating in a region associated with higher efficiencies for the duration of the drive cycle. The results therefore demonstrate that a balanced gear ratio between the two selected ratios is likely to achieve a more desirable result.

The primary uncertainty in this study is powertrain efficiency and additional losses that arise in the two-speed transmission, such as transmission and clutch drag or hydraulic fluid pumping, consume additional power from energy storage. Each of these losses is considered a single inefficiency in this paper, and through variation of this parameter the impact on vehicle performance for single speed and two-speed transmissions is demonstrated; see Figure 8. These results demonstrate that, as efficiency in the EM is very high over a broad range of operating conditions, it is difficult for the two-speed EV to significantly outperform the single speed EV in terms of driving range. Alternatively, driving performance in terms of vehicle acceleration demonstrates

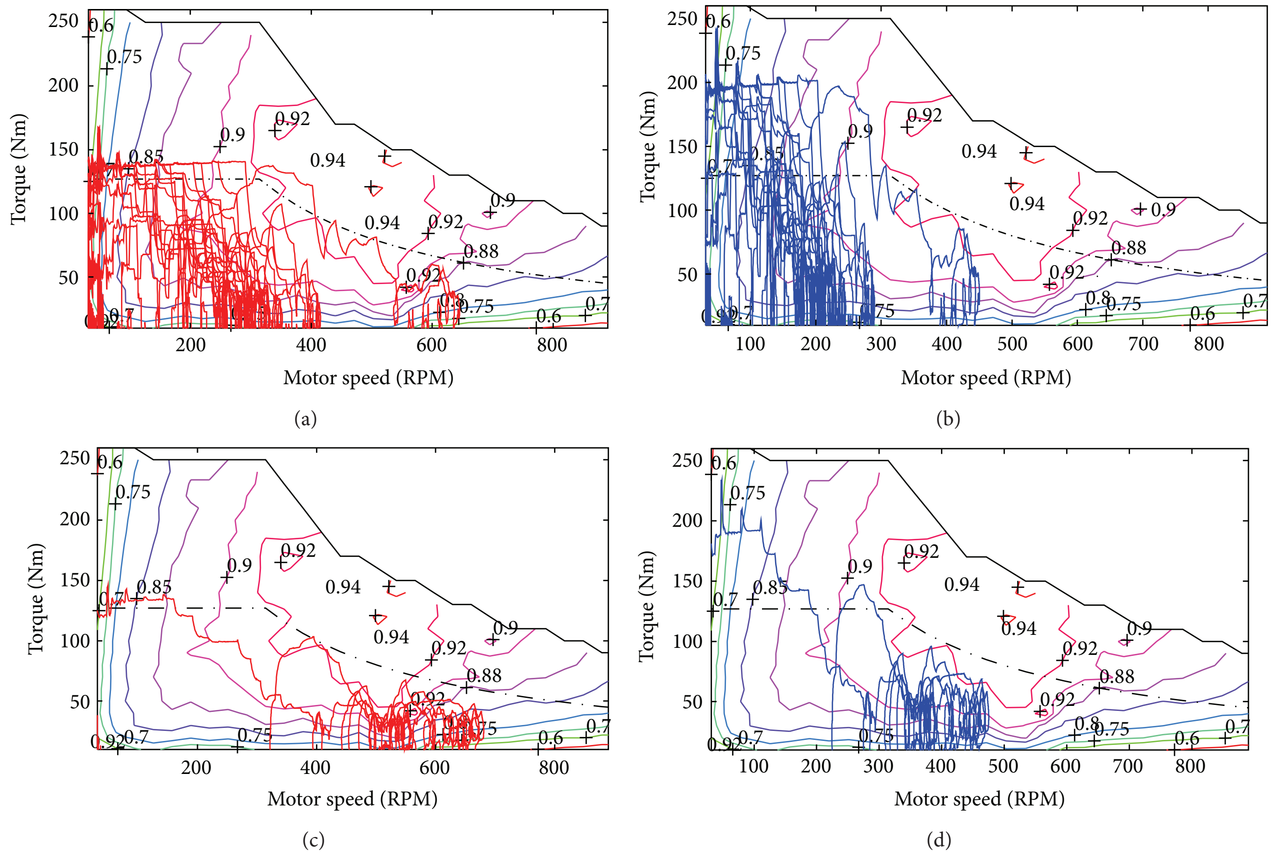

Figure 7: (a) Motor trace for UDDS cycle for a ratio of 8.17, (b) motor trace of UDDS cycles using a ratio of 5.7, (c) motor trace for HWFET cycle with a ratio of 8.17, and (d) motor trace of HWFET cycle using a ratio of 5.7.

significant benefits in the use of a two-speed EV across the range of applicable powertrain efficiencies.

5. Gear Ratio Optimisation through Genetic Algorithms

It is apparent from the presented results that it is not possible to reasonably achieve the desired performance specifications for single speed or two-speed EV powertrains through the direct selection of gear ratios. Alternative methods must therefore be sought for the identification of optimal gear ratios for each configuration. Generally, it is possible to apply a range of simulation based methods, such as parametric analysis, to determine optimal combination of gear ratios to provide desired performance and range capabilities. In this instance genetic algorithms (GA) are applied using model-in-the-loop simulations to determine optimal gear ratios for both powertrains and also shift schedule for the two-speed configuration. The major advantage of GA optimization is not a gradient based approach, and relatively little information is required to perform analysis. The downside of such techniques is that they are computationally intensive, with many simulations required to determine the optimal value.

Model based GA optimisation is an iterative process that uses simulation results to identify the best solution to complex design problems; it is summarised in Figure 9. Initially the user defines design variables and respective bounds and constraints. A range of possible solutions are determined from these variables and bounds and are evaluated using the model. Results are evaluated against constraints and convergence of the objective function is used to determine optimal design variables are reached. If convergence is not achieved, a range of better solutions are selected, bred, mutated, and recombined to determine a new range of variables within the best values, and the PEV powertrain model is evaluated again to get the new results for the objective function and the constraint functions. This process continues until the objective values converge and optimal results are achieved. See [21, 22] for detailed discussion on GA optimisation and its applications for further details.

5.1. Optimisation Design Variables and Constraints

5.1.1. Design Variables. If the intention of optimisation is to improve the acceleration performance, then the solution is quite obvious: push the transmission ratios to the upper limits to obtain maximum transmission output torque; this will always increase vehicle acceleration but at a cost of

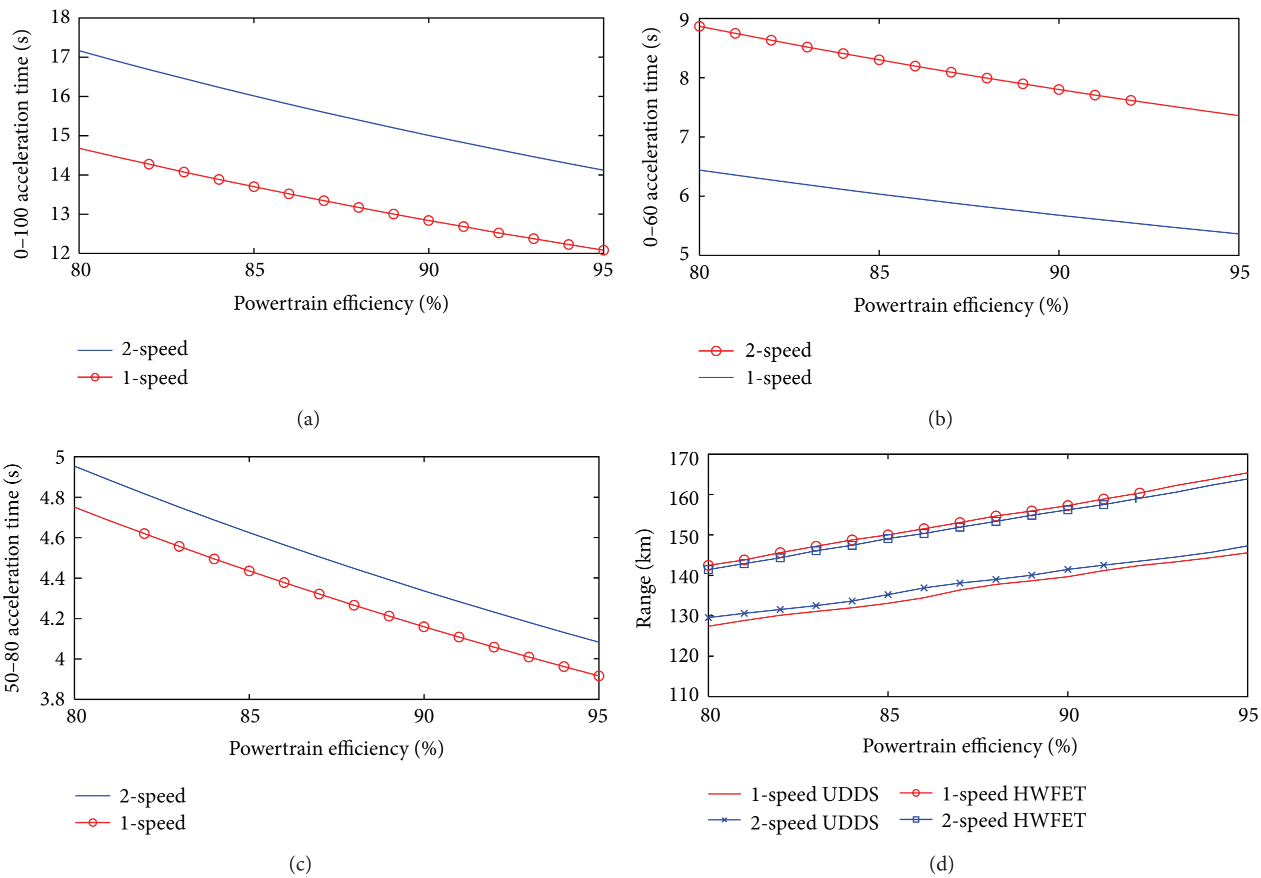

FIGURE 8: Influence of powertrain efficiency on vehicle performance: (a) 0–100 km/h acceleration, (b) 0–60 km/h acceleration, (c) 50–80 km/h acceleration, and (d) driving range for UDDS and HWFET drive cycles.

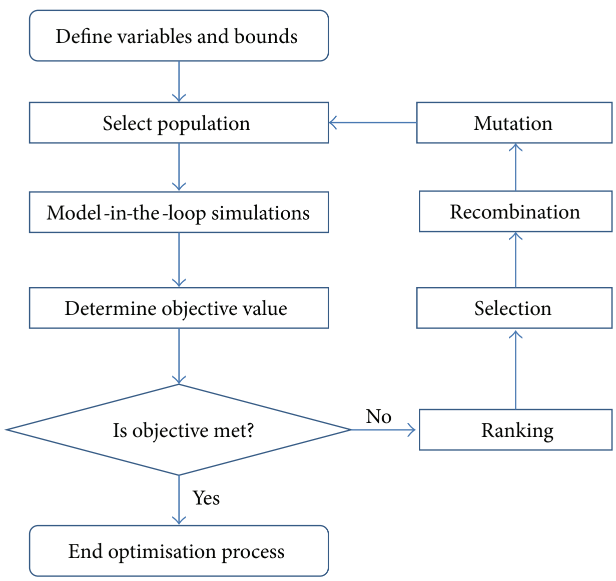

FIGURE 9: Genetic algorithm optimisation strategy.

range performance. Therefore, in targeting the ratio selection for optimisation the focus turns to maintaining vehicle range under desired performance constraints. The designed transmission ratios in Sections 3.1 and 3.2 for grade and top speed are the initial ratios for reference, but the design strategy employed also is applied to define the bounds of the available gear ratios. For the first gear the minimum ratio is defined by the grade requirement in (19). The maximum ratio, however, is designed using practical gearing requirements, where a ratio higher than 15 : 1 is difficult to produce even the two reduction ratios in the transmission and final drive. The second gear is bound by the minimum top speed designs as a function of both maximum motor speed and maximum torque at top speed; see (20) and (21). The ratios are then bound as follows:

$$8.17 \leq \gamma_1 \leq 15. \tag{24}$$

The maximum chosen ratio is therefore limited by available torque rather than top speed, and the bounds can be defined using a minimum ratio of 3.26 and a maximum of 5.7, eliminating overlap in the two ratios whilst enabling the powertrain to reach the minimum top speed of 150 kph:

$$3.26 \leq \gamma_2 \leq 5.7 \tag{25}$$

It should be noted here that the shift schedule for the two speed transmission will be unique to each ratio combination, as shifting points are distinct for each ratio combination.

For comparison, a single speed transmission is optimised to be compared with these results; thus a single design variable is provided for the overall speed ratio. For a single speed transmission it is necessary to trade between vehicle performance and top speeds. To achieve this, the bounds for the transmission ratio are set to be limited by grade climbing against top speed as follows:

$$5.7 \leq \gamma_1 \leq 8.17. \tag{26}$$

5.1.2. Constraints. For any vehicle, the two competing constraints that define vehicle design are range and performance. These are critical to electric vehicles to gain overall consumer acceptance. In (27)–(31) a series of vehicle specifications were defined as minimal goals for achieving an optimal design of the vehicle for acceptance. These parameters become the constraining properties for the PEV in the optimisation problem:

$$a_{100} \leq 14s, \tag{27}$$

$$a_{60} \leq 6.5s, \tag{28}$$

$$a_{50-80} \leq 5.5s, \tag{29}$$

$$\text{Grade} > 30\%, \tag{30}$$

$$V_{\max} > 150. \tag{31}$$

5.1.3. Objective Function. The objective function drives optimisation through maximising the mean motor efficiency and driving range during each of the two chosen drive cycles. For this problem the design variables are tuned to maximise range and mean motor efficiency during simulations under the previously described constraints. Thus, the optimisation process seeks to provide maximum range within the constrained design parameters. The objective function is defined as

$$f_{\mathrm{OBJ}} = \left(\frac{1}{N}\sum_{i=1}^{N}\eta_{\mathrm{EM}} + C_1 R\right)_{\mathrm{UDDS}} + \left(\frac{1}{N}\sum_{i=1}^{N}\eta_{\mathrm{EM}} + C_2 R\right)_{\mathrm{HWFET}}, \tag{32}$$

where N is a nonzero vehicle speed iteration of the simulation, R denotes range, and C_1 and C_2 are scaling constants to balance differing magnitudes between average efficiency and range with subscripts UDDS and HWFET denoting the respective drive cycles.

5.2. Optimisation Results. The described optimisation process is applied to the single speed and two-speed PEV powertrains for evaluation of driving range and vehicle performance with the primary intension of improving the two-speed vehicle performance characteristics in comparison to the single speed transmission. Performance, range, and efficiency results are summarised in Table 3 for both configurations and the best generation results of optimisation in Figure 10. These results demonstrate that for both transmissions the overall range improvement is rather limited resulting from the wide operating region of the electric machine.

Table 3: Vehicle performance results after optimization.

Parameter	Units	Transmission	
		One-speed	Two-speed
Optimised ratios	—	6.82	11.47, 4.64
Range HWFET	km	157.6	141.8
Mean motor efficiency HWFET	%	86	87.2
Range UDDS	km	142.1	130.4
Mean motor efficiency UDDS	%	79	80.2
Acceleration 0–100 km/h	s	13.48	13.49
Acceleration 0–60 km/h	s	6.48	5.22
Acceleration 50–80 km/h	s	4.18	4.61
Grade climbing	%	25	45
Top speed	Km/h	151	222

However the ability to achieve high quality performance outcomes for the single speed transmission is limited.

For the five constraints on the PEV powertrain listed in (27) to (31), top speed and grade climbing ability are either barely achieved or compromised in the optimisation process for the single speed transmission as a result of these constraints having competing relationships according to (19) and (20). The two-speed transmission either equals or outperforms the single speed in terms of vehicle performance characteristics for each constraint, with the exception of overtaking acceleration where gear change occurs during the manoeuvre reducing acceleration, thereby suggesting that the two-speed transmission benefits over a single speed transmission are primarily for enhancing vehicle performance rather than improving driving economy. However, it should be noted that the optimised two-speed transmission improves the mean motor efficiency for both chosen drive cycles, supporting the results in Figure 8 that suggest that the minimising of power losses in the two-speed transmission will further enhance range performance. It is therefore demonstrated that, as a result of the large operating region of the EM at efficiencies greater than 80%, it is difficult to achieve substantial performance improvement in the overall operating range of each vehicle. Thus limitations arise from optimization of the overall vehicle economic performance.

The influence of using an electric machine with high efficiency over a wide range of motor speeds and power is also demonstrated in Figure 10, where only small improvements are realised in the objective function; however results shown in Table 3 indicate significant improvements in results achieved for overall vehicle dynamic performance. For both optimisation processes each generation has a population of 30, thus demonstrating that with only one variable optimised the single speed transmission result is achieved in fewer simulation iterations.

Figures 11(a) to 11(d) present the operating points for the motor during both drive cycles for each of the optimisation cases presented in this paper for both UDDS and HWFET drive cycles. These results demonstrate that for the UDDS cycle the operating points for gear one are pushed into a

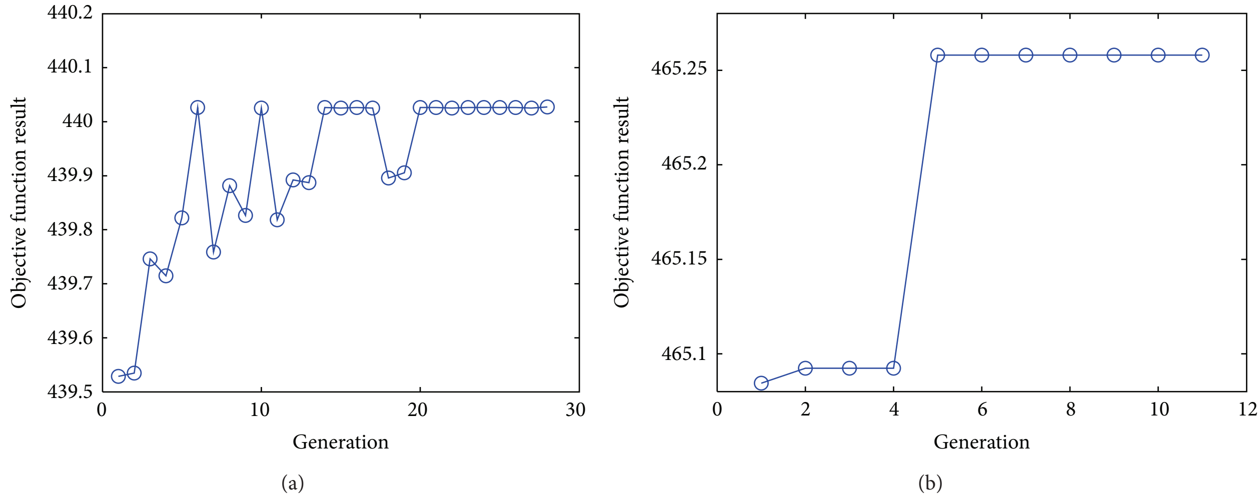

FIGURE 10: Objective function results for each generation during optimization.

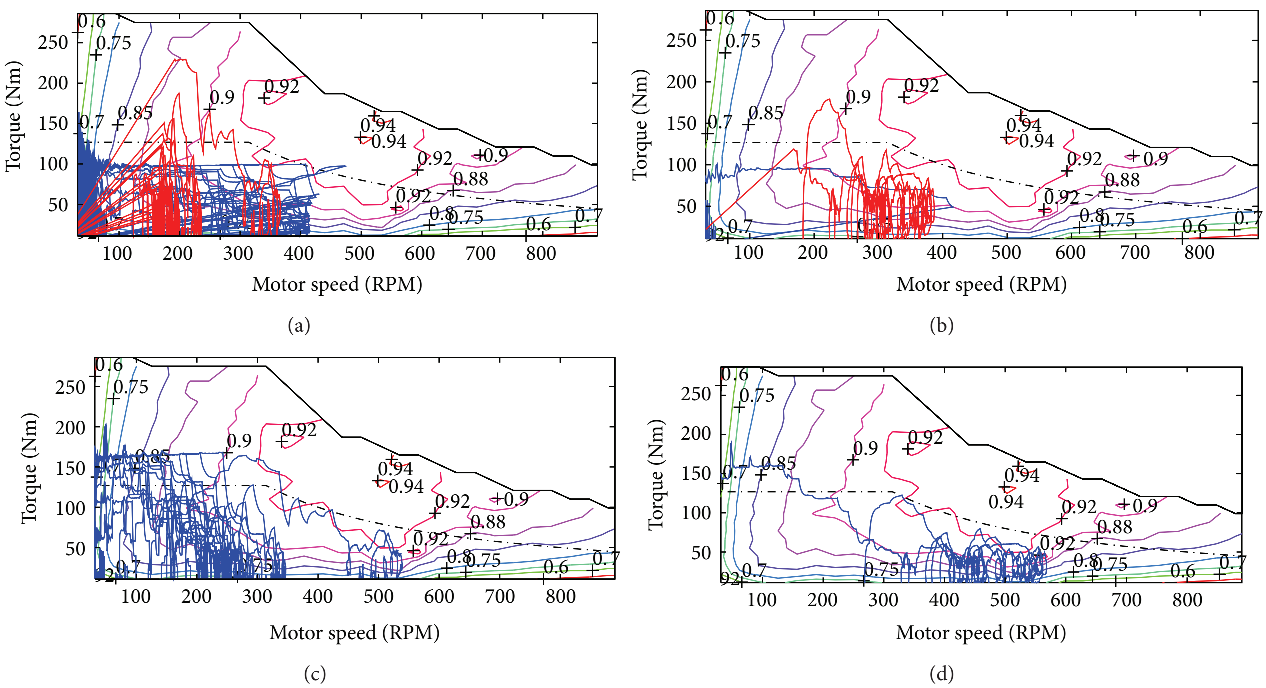

FIGURE 11: Motor efficiency maps and operating traces for (a) two-speed EV with UDDS cycle, (b) two speed EV with HWFET cycle, (c) one-speed EV with UDDS cycle, and (d) one-speed EV with HWFET cycle.

higher torque range at lower speed compared to Figure 5(c), as is the operating range when in second gear. Similarly, for the HWFET cycle in **Figure 11(b)** the operating region for gear 2 is reduced to a much lower region, less than 4000 RPM. These results demonstrate how the two-speed transmission works to improve the PEV driving range. When considered in comparison to a single speed transmission in Figures 11(c) and 11(d), results demonstrate the capability of the two-speed transmission to provide a much wider vehicle speed range at higher overall motor efficiencies when considered in comparison to single speed transmission results.

6. Conclusion

This paper presented a model based methodology for the design and analysis of multispeed electric vehicle powertrains, with particular focus on the analysis of the impact of gear ratio selection on vehicle performance and economy. Through system level powertrain design it is possible to investigate a range of design parameters and how, through simulation, these parameters influence a range of vehicle characteristics such as driving range or acceleration performance. Probably the most important consideration in terms of vehicular range and performance is powertrain efficiency; in this paper it is identified as a significant source of uncertainty in the analysis and is treated conservatively to illustrate the differences between the two transmission options. Detailed design study in future research for two-speed transmission configurations will provide a more precise estimate of both powertrain efficiencies and improve results achieved herein. The design of transmission ratios for grade climbing and top speed was considered, and the effect of applying these ratios on the vehicles applicable traction force range is demonstrated. Results of simulations demonstrate that improved grade climbing, acceleration, and top speed are achieved through the application of a multispeed transmission. Thus, vehicle performance is heavily dependent on transmission design for PEVs. However the economic performance, that is, energy consumption, is weakly influenced by transmission ratio selection. Alternatively, in a single speed transmission there is a difficult balance required to ensure that efficiency, acceleration, and top speed performance characteristics can be successfully achieved.

Additionally, genetic algorithm optimisation was applied using model-in-the-loop techniques to determine the optimised gear ratio for single speed and two-speed transmissions in PEVs. These results demonstrated that, while it is possible to achieve an optimal single speed and two-speed transmission ratios for maximum vehicle range, the variation in driving range is very weakly associated with gear ratios. Performance constraints placed on the vehicle during optimisation are difficult to achieve for a single speed transmission. Nevertheless, it is clearly demonstrated that the application of two-speed transmission to PEVs has the effect of improving vehicle performance for top speed, grade climbing, and acceleration without substantially compromising driving range in comparison to single speed PEVs.

Conflict of Interests

The authors declare that there is no conflict of interests regarding the publication of this paper.

Acknowledgments

This project is supported by BAIC Motor Electric Vehicle Co. Ltd., the Ministry of Science and Technology, China, and University of Technology, Sydney.

References

[1] M. Kamachi, H. Miyamoto, and Y. Sano, "Development of power management system for electric vehicle 'i-MiEV'," in *Proceeding of the International Power Electronics Conference (IPEC '10)*, pp. 2949–2955, Sapporo, Japan, June 2010.

[2] A. R. Salisa, N. Zhang, and J. Zhu, "Recent advancements in management of hybrid vehicle powertrains," in *Proceeding of the International Conference of Sustainable Automotive Technologies (ICSAT '08)*, pp. 1–4, Melbourne, Australia, 2008.

[3] N. Jinrui, W. Zhifu, and R. Qinglian, "Simulation and analysis of performance of a pure electric vehicle with a super capacitor," in *Proceeding of the IEEE Vehicle Power and Propulsion Conference (VPPC '06)*, pp. 1–6, Windsor, UK, September 2006.

[4] J. P. Trovao, P. G. Pereirinha, and F. J. T. E. Ferreira, "Comparative study of different electric machines in the powertrain of a small Electric Vehicle," in *Proceeding of the 18th International Conference on Electrical Machines (ICEM '08)*, pp. 1–6, Vilamoura, Portugal, September 2008.

[5] M. Eberhard and M. Tarpenning, "The 21st century electric car," Tesla Motors White Paper, 2006, http://www.fcinfo.jp/whitepaper/687.pdf.

[6] A. R. Salisa, N. Zhang, and J. Zhu, "A comparative analysis of fuel economy and emissions between a conventional HEV and the UTS PHEV," *IEEE Transactions on Vehicular Technology*, vol. 60, no. 1, pp. 44–54, 2011.

[7] S. Zhang, G. Wu, and S. Zheng, "Study on the energy management strategy of DCT-based series-parallel PHEV," in *Proceeding of the 1st International Conference on Computing Control and Industrial Engineering (CCIE '10)*, pp. 25–29, Wuhan, China, June 2010.

[8] A. C. Baisden and A. Emadi, "ADVISOR-based model of a battery and an ultra-capacitor energy source for hybrid electric vehicles," *IEEE Transactions on Vehicular Technology*, vol. 53, no. 1, pp. 199–205, 2004.

[9] S. Bogosyan, M. Gokasan, and D. J. Goering, "A novel model validation and estimation approach for hybrid serial electric vehicles," *IEEE Transactions on Vehicular Technology*, vol. 56, no. 4, pp. 1485–1497, 2007.

[10] L. Fang, S. Qin, G. Xu, T. Li, and K. Zhu, "Simultaneous optimization for hybrid electric vehicle parameters based on multi-objective genetic algorithms," *Energies*, vol. 4, no. 3, pp. 532–544, 2011.

[11] C. C. Chan, A. Bouscayrol, and K. Chen, "Electric, hybrid, and fuel-cell vehicles: architectures and modeling," *IEEE Transactions on Vehicular Technology*, vol. 59, no. 2, pp. 589–598, 2010.

[12] A. Rousseau, S. Pagerit, and D. W. Gao, "Plug-in hybrid electric vehicle control strategy parameter optimization," *Journal of Asian Electric Vehicles*, vol. 6, no. 2, pp. 1125–1133, 2008.

[13] L. C. Fang and S. Y. Qin, "Concurrent optimization for parameters of powertrain and control system of hybrid electric vehicle based on multi-objective genetic algorithms," in *Proceeding of the International Joint Conference (SICE-ICASE '06)*, pp. 2424–2429, Busan, Republic of Korea, October 2006.

[14] B. Zhang, Z. Chen, C. Mi, and Y. L. Murphey, "Multi-objective parameter optimization of a series hybrid electric vehicle using evolutionary algorithms," in *Proceeding of the IEEE Vehicle Power and Propulsion Conference (VPPC '09)*, pp. 921–925, Dearborn, Mich, USA, September 2009.

[15] C. N. Shiau, N. Kaushal, C. T. Hendrickson, S. B. Peterson, J. F. Whitacre, and J. J. Michalek, "Optimal plug-in hybrid electric vehicle design and allocation for minimum life cycle cost, petroleum consumption, and greenhouse gas emissions," *Journal of Mechanical Design*, vol. 132, no. 9, Article ID 091013, 11 pages, 2010.

[16] Y. Zhu, Y. Chen, Z. Wu, and A. Wang, "Optimisation design of an energy management strategy for hybrid vehicles," *International Journal of Alternative Propulsion*, vol. 1, no. 1, pp. 47–62, 2006.

[17] V. H. Johnson, K. B. Wipke, and D. J. Rausen, "HEV control strategy for real-time optimization of fuel economy and emissions," SAE Technical Paper 2000-01-1543, 2000.

[18] M. Ceraolo, A. Donato, and G. Franceschi, "A general approach to energy optimization of hybrid electric vehicles," *IEEE Transactions on Vehicular Technology*, vol. 57, no. 3, pp. 1433–1441, 2008.

[19] G. Lechner and H. Naunheimer, *Automotive Transmissions—Fundamentals, Selection, Design and Application* , Springer, Berlin, Germany, 1999.

[20] M. A. Kluger and D. M. Long, "An overview of current automatic, manual and continuously variable transmission efficiencies and their projected future improvements," SAE Technical Paper 1999-01-1259.

[21] K. Deb, "Multi-objective optimisation using evolutionary algorithms: an introduction," in *Multi-Objective Evolutionary Optimisation for Product Design and Manufacturing*, L. Wang and A. H. C. Ng, Eds., pp. 3–35, Springer, London, UK, 2011.

[22] X. Yu and M. Gen, *Introduction to Evolutionary Algorithms*, Springer, London, UK, 2010.